

High field magneto-transmission investigation of natural graphite

N. Ubrig,¹ P. Plochocka,² P. Kossacki,² M. Orlita,² D. K. Maude,² O. Portugall,¹ and G. L. J. A. Rikken^{1,2}

¹Laboratoire National des Champs Magnétiques Intenses, CNRS-UJF-UPS-INSA, 31400 Toulouse, France

²Laboratoire National des Champs Magnétiques Intenses, CNRS-UJF-UPS-INSA, 38042 Grenoble, France

(Dated: April 22, 2022)

Magneto-transmission measurements in magnetic fields in the range $B = 20 - 60$ T have been performed to probe the H and K -point Landau level transitions in natural graphite. At the H -point, two series of transitions, whose energy evolves as \sqrt{B} are observed. A reduced Slonczewski, Weiss and McClure (SWM) model with only two parameters to describe the intra-layer (γ_0) and inter-layer (γ_1) coupling correctly describes all observed transitions. Polarization resolved measurements confirm that the observed apparent splitting of the H -point transitions at high magnetic field cannot be attributed to an asymmetry of the Dirac cone.

PACS numbers: 81.05.uf, 71.70.Di, 78.20.Ls, 78.30.-j

Graphite consists of Bernal stacked sheets of hexagonally arranged carbon atoms. The weak coupling between the layers transforms the single graphene layer, which is a gapless semiconductor with a linear dispersion, into a semimetal with electron and hole puddles along the $H - K - H$ edge of the hexagonal Brillouin zone.¹ In a magnetic field the electronic structure of graphite is accurately described by the Slonczewski, Weiss and McClure (SWM) band structure calculations,^{2,3} which require seven tight binding parameters $\gamma_0, \dots, \gamma_5, \Delta$ to define the interaction energy of the carbon atoms in the graphite lattice. The SWM model has been extensively verified using Shubnikov de Haas, de Haas van Alphen, thermopower and magneto-reflectance experiments.⁴⁻¹¹ Carriers at the H -point behave as relativistic Dirac Fermions with a linear dispersion as in graphene. Magneto-absorption has been used to perform Landau level spectroscopy of carriers at the H -point ($k_z = 0.5$) and K -point ($k_z = 0$) in both natural graphite and highly ordered pyrolytic graphite (HOPG).¹²⁻¹⁵

At the H -point, transitions with a characteristic \sqrt{nB} magnetic field dependence of their energy are observed, which are identical to the transitions at the K and K' -points observed in graphene. For this reason, we refer to this series as “graphene-like” although we stress that here the series arises from the H -point transitions of perfect bulk graphite. In addition, a second weaker series of transitions with a characteristic \sqrt{nB} magnetic field dependence of their energy are observed. These transitions are absent in graphene, in fact they correspond to dipole forbidden transitions of the “graphene-like” series. However, this series correspond to dipole allowed transitions in graphite due to the complicated band structure at the H -point.^{13,16,17} We refer to these transitions as the “graphite-like” series, since they are absent in graphene. For the K -point there is evidence of a splitting of the transitions which has been attributed to electron-hole asymmetry.¹⁵

Here we report magneto-optical absorption measurements to probe the evolution of the K and H point transitions in magnetic fields up to 60 T. This extends previous work¹²⁻¹⁵ to higher magnetic fields and more

importantly to higher energies. In particular, the use of near visible radiation facilitates the implementation of polarization resolved measurements. The observed transmission spectra are dominated by the Dirac-like series of transitions from the H -point. All the observed transitions can be assigned, and the magnetic field evolution reproduced, using a reduced SWM model with two tight binding parameters γ_0 and γ_1 . Polarization resolved measurements confirm that the observed splitting of the H -point “graphene-like” transitions is not linked to the asymmetry of the Dirac cone, which is anyway irrelevant at the H -point within the SWM model. Upon closer examination, the splitting resembles rather an avoided level crossing, while nevertheless remaining unexplained.

Thin samples for the transmission measurements were prepared by exfoliating natural graphite. The average thickness of the graphite layers remaining on the foil was estimated to be $\simeq 100$ nm.¹³ The measurements were performed up to 34 T at the dc resistive magnet laboratory in Grenoble and up to 60 T at the pulsed magnetic field laboratory in Toulouse. For the absorption measurements a tungsten halogen lamp was used to provide broad spectrum in the visible and near infra-red range. The absorption was measured in the Faraday configuration in which k , the wave propagation vector is parallel to the magnetic field, B . The c -axis of the graphite sample was parallel to magnetic field. A nitrogen cooled InGaAs photodiode array coupled to a spectrometer collected the transmitted light from the sample in the spectral range 850 – 1600 nm, *i.e.* energies of 0.8 – 1.5 eV. For the pulsed field measurements the exposure time was limited to 2 ms in order to limit variations in the magnetic field during acquisition. Thirty spectra were taken during a 60 T shot so that in principle a complete magnetic field dependence can be acquired in a single shot. The magnetic field was systematically measured using a calibrated pick-up coil. Since the absorption lines in this energy range are weak all the spectra were normalized by the zero field transmission to produce a differential transmission spectra.

Typical differential magneto-absorption spectra measured at $T = 4.2$ K for magnetic fields 48 – 58 T are

shown in Figure 1(a). All spectra show a number of absorption lines which can be assigned to dipole allowed transitions at the H and K points. The energetic position of the observed absorption lines is plotted as a function of the magnetic field in Figure 1(b). In order to assign the transitions we first calculate the energy of the dipole allowed transitions ($\Delta n = \pm 1$) at the H and K -points using a greatly simplified SWM model with only two parameters γ_0 and $\lambda\gamma_1$ to describe the intra- and inter-layer coupling.^{14,15,18–20} Here $\lambda = 2 \cos(\pi k_z)$ and k_z is the momentum perpendicular to the layers. This corresponds to treating graphite as a series of graphene bi-layers whose effective coupling depends on k_z . The magneto-optical response is dominated by the singularities in the joint density of initial and final states which occur at the K -point ($\lambda = 2$) and H -point ($\lambda = 0$). The energy spectrum of the Landau levels using the effective bilayer model is then given by,

$$E_{3\pm}^n = \pm \frac{1}{\sqrt{2}} \left[(\lambda\gamma_1)^2 + (2n+1)\varepsilon^2 - \sqrt{(\lambda\gamma_1)^4 + 2(2n+1)\varepsilon^2(\lambda\gamma_1)^2 + \varepsilon^4} \right]^{1/2}, \quad (1)$$

where $\varepsilon = \tilde{c}\sqrt{2e\hbar B}$ is the characteristic magnetic energy, $\tilde{c} = \sqrt{3}ea_0\gamma_0/2\hbar$ is the Fermi velocity, $a_0 = 0.246$ nm is the lattice constant in the ab plane and \pm labels the electron and hole Landau levels respectively. At the H -point, equation (1) reduces to the Landau level spectrum of graphene with $E_{3\pm}^n = \pm\tilde{c}\sqrt{2e\hbar B}n$.

The bi-layer model is expected to be almost exact at the H -point since the effect of trigonal warping (γ_3) vanishes and analytic expressions for the Landau levels can be easily obtained within the SWM model by diagonalizing the Hamiltonian.¹⁶ However, the situation is complicated by the presence of the E_1 and E_2 bands (see Fig.2), which are almost degenerate with E_3 at the H -point (energy splitting $\Delta \simeq -0.007$ eV). In a magnetic field, neglecting the two exceptional E_3 Landau levels ($n = 0, -1$), this gives rise to a second Landau level spectrum, $E_{1,2}^n = E_{3\pm}^{n+1}$ where $n = 1, 2, 3, \dots$ which is exactly degenerate with the $E_{3\pm}$ ladder.^{13,14,16} The Landau level spectrum at the H -point is shown schematically in Fig. 2 where we indicate all possible dipole allowed $E^{2(3)} \rightarrow E^{3(2)}$ transitions as an example. The graphene like transition $E_{3-}^{3(2)} \rightarrow E_{3+}^{2(3)}$ (labeled D) have the same energy as the $E_2^{2(1)} \rightarrow E_1^{1(2)}$ transitions which have a quantum number n which is lower by one. The circular polarization of the light required to excite each transition is indicated and we have adopted the convention that σ^+ polarization corresponds to $\Delta n = +1$. The transition labeled d and d' are specific to graphite (“graphite-like” series). Transition d is the dipole allowed ($|\Delta n| = 1$) degenerate ‘mixed’ transitions $E_{3-}^3 \rightarrow E_1^2$ and $E_2^2 \rightarrow E_{3+}^3$ which correspond to (are exactly degenerate with) dipole forbidden ($\Delta n = 0$) transitions of the graphene series. Transition d' shows dipole allowed ($|\Delta n| = 1$) degenerate ‘mixed’ transitions $E_{3-}^3 \rightarrow E_1^3$ and $E_2^2 \rightarrow E_{3+}^2$ which

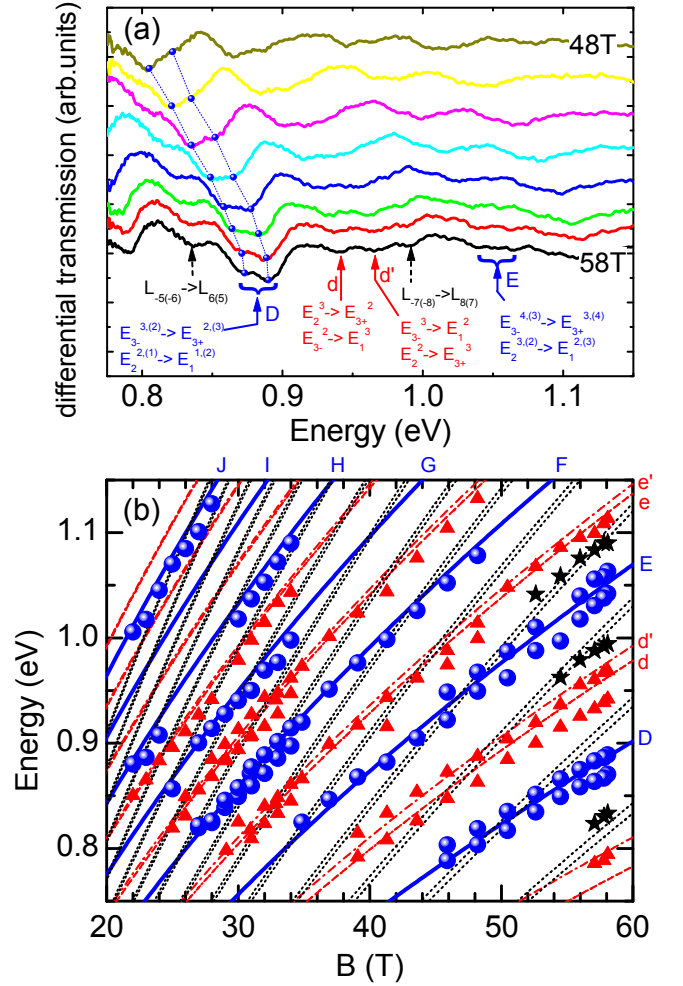


FIG. 1: (Color online) (a) Typical differential magneto-transmission spectra of natural graphite measured at magnetic fields in the range 48 – 58 T at $T = 4.2$ K. (b) Magnetic field dependence of the observed transitions assigned as follows: H -point, graphene series (blue balls), graphite specific series (red triangles); K -point (black stars). The lines are calculated energies of the dipole allowed H -point (solid, dotted, and, dot-dashed lines) and K point (dashed lines) transitions as described in the text.

correspond to (are exactly degenerate with) dipole forbidden transitions $|\Delta n| = 2$ of the graphene series. Note, that while we cannot exclude the presence in our sample of decoupled graphene layers, with transitions degenerate with the “graphene-like” series, the overwhelming contribution of graphite to the transmission is demonstrated by the observed strength of the “graphite-like” series.

The energy of the dipole allowed optical transitions, calculated using Equation(1) with the tight binding parameters, $\gamma_0 = 3.15$ eV ($\tilde{c} = 1.02 \times 10^6$ m.s⁻¹) and $\gamma_1 = 0.375$ eV determined from magneto-absorption measurements at lower magnetic fields,¹⁴ are plotted as a function of the magnetic field in Fig. 1(b) (solid and broken lines). The H -point transitions depend only on

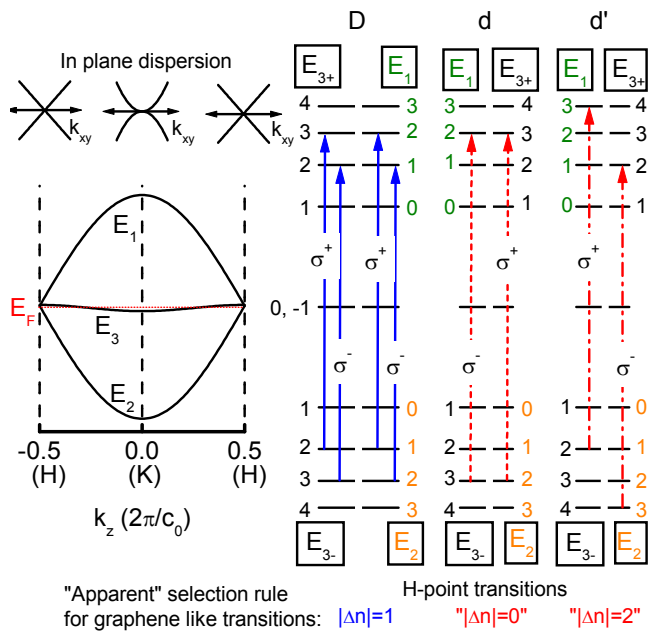


FIG. 2: (Color online) (left) Band structure of graphite along the hexagonal $H-K-H$ axis. (right) Dipole allowed transitions ($\Delta n = 1$) in a magnetic field at the H -point corresponding the $E_{3-} \rightarrow E_{3+}$ (and $E_2 \rightarrow E_1$) “graphene-like” transitions (labeled D), and the ‘mixed’ $E_{3-} \rightarrow E_2$ and $E_2 \rightarrow E_{3+}$ “graphite-like” transitions (labeled d and d'). The circular polarization required to excite each transition is indicated using the convention that σ^+ polarization corresponds to $\Delta n = +1$.

the parameter γ_0 and evolve always as \sqrt{B} . The K -point transition depend also on the inter-layer coupling $\lambda\gamma_1$, and therefore, as can be seen from Equation(1), evolve linearly at low energy ($\varepsilon \ll \lambda\gamma_1$) before increasing as \sqrt{B} at high energies ($\varepsilon \gg \lambda\gamma_1$). At the K -point $\lambda\gamma_1 = 0.75$ eV so that we are in the intermediate regime where dependence is somewhere between linear and \sqrt{B} .

The agreement between the reduced two-parameter SWM model and experiment in Figure 1(b) is remarkable, especially taking into account that there are no adjustable parameters. The H -point transitions $E^{2(3)} \rightarrow E^{3(2)}$, are labeled as in Fig.2. Mainly H -point transitions are observed, notably the “graphene-like” series $E_{3-} \rightarrow E_{3+}$ and $E_2 \rightarrow E_1$ (thick blue solid lines labeled with upper case letters) together with the weaker $E_{3-} \rightarrow E_1$ and $E_2 \rightarrow E_{3+}$ transitions (red dashed and dot-dashed lines labeled with lower case letters). The K -point transitions, shown as black dotted lines are only observed directly at high magnetic fields. For completeness, for the K -point transitions, we have included phenomenologically the electron-hole asymmetry as suggested in Refs.[15,21] by using a different Fermi velocity $\tilde{c}_e = 1.098 \times 10^6$ ms $^{-1}$ and $\tilde{c}_h = 0.942 \times 10^6$ ms $^{-1}$ for the electrons and holes respectively. These values are slightly different from those used in Ref.15 in order to have the same “average” value of $\gamma_0 = 3.15$ eV. While

the electron-hole asymmetry was clearly seen in measurements at low magnetic field,¹⁵ the phenomenological asymmetry splitting introduced in Ref.[15] decreases rapidly with increasing quantum number, and is probably too small to be seen in our high magnetic field data (the lowest energy K -point transition seen is $n = 5$, labeled $L_{-5(-6)} \rightarrow L_{6(5)}$ in Figure 1(a)).

The “graphene-like” series unexpectedly shows what looks at first sight to be a splitting, which is puzzling since such a splitting is completely absent in magneto-transmission measurements on graphene.²² This apparent splitting is clearly seen in the $E_{3-}^{n(n+1)} \rightarrow E_{3+}^{n+1(n)}$ transitions ($n = 2, 3, 4$) labeled D, E and F in Fig.1. However, a closer inspection of the magnetic field evolution of the energy of the strong $E_{3-}^{2(3)} \rightarrow E_{3+}^{3(2)}$ in Fig. 1(b) (transition D) indicates that the calculated transition fits better to the low energy feature at low fields ($B < 50$ T) before fitting better to the high energy feature at high fields ($B > 54$ T). This is suggestive of an avoided level crossing rather than a splitting. This hypothesis is supported by the absorption spectra in Fig. 1(a), where it is clearly seen that the $E_{3-}^{2(3)} \rightarrow E_{3+}^{3(2)}$ doublet (transition D) consists of a stronger low energy transition at low magnetic fields which switches to a stronger high energy feature at high fields, *i.e.* the two lines anti-cross. The origin of this behavior remains to be elucidated. However, this cannot be due to inhomogeneity of the sample. A slightly different Fermi velocity for different regions would simply lead to an increased splitting with increasing magnetic field.

Figure 3(a) shows differential absorption spectra measured at $B = 58$ T for different temperatures in the range 4 – 300 K. A temperature of 100 K is already sufficient to suppress the apparent splitting of the $E_{3-}^{2(3)} \rightarrow E_{3+}^{3(2)}$ transition, although the transition itself, while weakening slightly, remains clearly visible even at room temperature. The $T = 4$ K spectra have been fitted using a Lorentzian line shape of full width at half maximum (FWHM) of 28.5 meV for all transitions. The result of the fit (solid thin black line in Fig.3(a)) describes the data extremely well. The individual Lorentzians, for each transition are shown as dotted lines. Clearly, the broadening of the transitions is comparable to the energy separation so that the absorption is only weakly modulated. Note that the disagreement between the data and the fit around 0.92 eV is probably a signature of the “missing” $L_{-6(-7)} \rightarrow L_{7(6)}$ K -point transition in Fig.1 which could not be assigned from the raw data. Keeping all other parameters constant, increasing the broadening of the Lorentzians produces a reasonable fit to the higher temperature data, with the exception of the $E_{3-}^{2(3)} \rightarrow E_{3+}^{3(2)}$ transition. A reasonable fit to this transition at higher temperatures requires, in addition to a thermal broadening, that the amplitude of the two Lorentzian components be changed for which we see no physical justification. We therefore conclude that thermal broadening alone cannot explain the observed temperature depen-

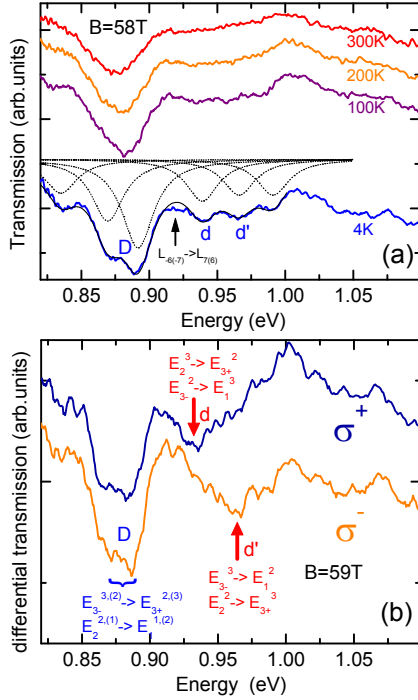


FIG. 3: (Color online) (a) Differential magneto-transmission spectra of natural graphite measured at $B = 58$ T for different temperatures. The thin black lines are a fit to the $T = 4$ K spectra assuming a Lorentzian line shape. (b) Polarization resolved spectra measured at $B = 59$ T and $T = 4.2$ K for the transitions D , d and d' sketched schematically in Fig. 2. The polarization (σ^+ or σ^-) has been arbitrarily assigned to a given magnetic field direction.

dence of the $E_{3-}^{2(3)} \rightarrow E_{3+}^{3(2)}$ transition.

From a theoretical point of view a splitting of the $E_{3-}^{2(3)} \rightarrow E_{3+}^{3(2)}$ transition (or the degenerate $E_2^{1(2)} \rightarrow E_1^{2(1)}$ transition) is not expected since even in the full SWM model. The effect of γ_3 (trigonal warping) vanishes at the H -point so that the energy levels are determined only by γ_0 . The non vertical inter layer coupling term γ_4 , which induces electron-hole asymmetry, plays no role. This can be verified experimentally using the polarization resolved absorption measured at 59 T shown in Fig. 3(b) which focuses on transitions D , d and d' . There is no difference between σ^+ and σ^- spectra for $E_{3-}^{2(3)} \rightarrow E_{3+}^{3(2)}$ (transition D) confirming that the apparent doublet cannot under any circumstances be assigned to electron-hole asymmetry. In contrast, the ‘mixed’ $E_{3-} \rightarrow E_1$ and $E_2 \rightarrow E_{3+}$ transitions (d and d') show a marked dependence on the circular polarization with one of the transitions almost vanishing with either σ^+ or σ^- excitation. Using the polarization selection rules sketched in Fig.2 this can be explained provided one of the inter-band transitions ($E_{3-} \rightarrow E_1$ or $E_2 \rightarrow E_{3+}$) dominates.

However, as in our experiment the sense of the circular polarization has been arbitrarily assigned to a given magnetic field direction it is unfortunately not possible to know which transition prevails.

While trigonal warping plays no role at the H -point because γ_3 always enters the SWM Hamiltonian as $\gamma_3 \cos(\pi k_z)$, close to the H -point it can lead to magnetic breakdown producing a splitting of levels in the Landau level structure which could possibly be observed in magneto-optical spectra at the H -point.¹⁶ This originates from an anti-crossing of Landau levels from the E_3 band with Landau levels from the E_1 or E_2 bands. The repulsion occurs due to the interaction caused by γ_3 provided the Landau levels originate from the same sub-matrix (of the three possible) of the magnetic Hamiltonian. In contrast to the K -point, where trigonal warping induced magnetic breakdown occurs only at low magnetic fields, close to the H -point magnetic breakdown takes place for all magnetic field strengths. An additional complication at very high magnetic fields ($B \approx 70$ T) is the predicted magnetic field induced transition of semi-metallic graphite to a zero gap semiconductor due to the crossing of the $n = 0$ Landau level at the K -point and the $n = -1$ Landau level at the H -point.¹⁶ Further measurements at higher magnetic fields are planned to clarify these issues.

In conclusion, magneto-transmission measurements have been used to probe the H and K -point Landau level transitions in natural graphite. In the magnetic field range investigated, the spectra are dominated by transitions at the H -point. A ‘‘graphene-like’’ series together with a series of transitions exclusive to graphite are observed. We stress that both series arise from dipole allowed transitions at the H -point of *perfect bulk graphite*, and do not require the presence of decoupled graphene layers or decoupled bilayers in the sample. A reduced SWM model with only two parameter γ_0 and γ_1 correctly describes all observed transitions. Polarization resolved measurements (i) confirm that the apparent splitting of the ‘‘graphene-like’’ series at high magnetic field cannot be attributed to an asymmetry of the Dirac cone and (ii) suggest that the matrix elements connecting $E_{3+} \rightarrow E_1$ and $E_{3-} \rightarrow E_2$ are very different.

Acknowledgments

This work has been partially supported by ANR contract PNANO-019-06, Euromagnet II and grant GACR P204/10/1020. The authors thank Sylvie George and the LNCMI machine shops for technical support. Two of us (P.P. and P.K.) are financially supported by the EU under FP7, contract no. 221249 ‘SESAM’ and contract no. 221515 ‘MOCNA’ respectively.

-
- ¹ P. R. Wallace, Phys. Rev. **71**, 9 (1947).
 - ² J. C. Slonczewski and P. R. Weiss, Phys. Rev. **109**, 272 (1958).
 - ³ J. W. McClure, Phys. Rev. **119**, 606 (1960).
 - ⁴ D. E. Soule, Phys. Rev. **112**, 698 (1958).
 - ⁵ D. E. Soule, J. W. McClure, and L. B. Smith, Phys. Rev. **134**, A453 (1964).
 - ⁶ J. A. Woollam, Phys. Rev. Lett. **25**, 810 (1970).
 - ⁷ J. A. Woollam, Phys. Rev. B **3**, 1148 (1971).
 - ⁸ J. M. Schneider, M. Orlita, M. Potemski, and D. K. Maude, Phys. Rev. Lett. **102**, 166403 (2009).
 - ⁹ Z. Zhu, H. Yang, B. Fauqué, Y. Kopelevich, and K. Behnia, Nature Physics **6**, 26 (2010).
 - ¹⁰ S. J. Williamson, S. Foner, and M. S. Dresselhaus, Phys. Rev. **140**, A1429 (1965).
 - ¹¹ P. R. Schroeder, M. S. Dresselhaus, and A. Javan, Phys. Rev. Lett. **20**, 1292 (1968).
 - ¹² R. E. Doezema, W. R. Datars, H. Schaber, and A. Van Schyndel, Phys. Rev. B **19**, 4224 (1979).
 - ¹³ M. Orlita, C. Faugeras, G. Martinez, D. K. Maude, M. L. Sadowski, and M. Potemski, Phys. Rev. Lett. **100**, 136403 (2008).
 - ¹⁴ M. Orlita, C. Faugeras, J. M. Schneider, G. Martinez, D. K. Maude, and M. Potemski, Phys. Rev. Lett. **102**, 166401 (2009).
 - ¹⁵ K.-C. Chuang, A. M. R. Baker, and R. J. Nicholas, Phys. Rev. B **80**, 161410 (2009).
 - ¹⁶ K. Nakao, J. Phys. Soc. Japan **40**, 761 (1976).
 - ¹⁷ W. W. Toy, M. S. Dresselhaus, and G. Dresselhaus, Phys. Rev. B **15**, 4077 (1977).
 - ¹⁸ B. Partoens and F. M. Peeters, Phys. Rev. B **74**, 075404 (2006).
 - ¹⁹ B. Partoens and F. M. Peeters, Phys. Rev. B **75**, 193402 (2007).
 - ²⁰ M. Koshino and T. Ando, Phys. Rev. B **77**, 115313 (2008).
 - ²¹ E. A. Henriksen, Z. Jiang, L.-C. Tung, M. E. Schwartz, M. Takita, Y.-J. Wang, P. Kim, and H. L. Stormer, Phys. Rev. Lett. **100**, 087403 (2008).
 - ²² P. Plochocka, C. Faugeras, M. Orlita, M. L. Sadowski, G. Martinez, M. Potemski, M. O. Goerbig, J.-N. Fuchs, C. Berger, and W. A. de Heer, Phys. Rev. Lett. **100**, 087401 (2008).